

Cambridge University Press

978-1-107-41356-6 - In Situ Process Diagnostics and Intelligent Materials Processing

Edited by Peter A. Rosenthal, Walter M. Duncan and John A. Woollam

Excerpt

[More information](#)

Part I

**Sensor Technologies and
Semiconductor Diagnostics**

Cambridge University Press

978-1-107-41356-6 - In Situ Process Diagnostics and Intelligent Materials Processing

Edited by Peter A. Rosenthal, Walter M. Duncan and John A. Woollam

Excerpt

[More information](#)

Cambridge University Press

978-1-107-41356-6 - In Situ Process Diagnostics and Intelligent Materials Processing

Edited by Peter A. Rosenthal, Walter M. Duncan and John A. Woollam

Excerpt

[More information](#)**REAL-TIME MONITORING OF SEMICONDUCTOR GROWTH BY SPECTROSCOPIC ELLIPSOMETRY**

B. JOHS*, J. HALE*, C. HERZINGER*, D. DOCTOR**, K. ELLIOTT**, G. OLSON**, D. CHOW**, J. ROTH**, I. FERGUSON***, M. PELCZYNSKI***, C.H. KUO****, AND S. JOHNSON*****

* J.A. Woollam Co., Inc., 645 M St. #102, Lincoln, NE 68508, bjohs@jawoollam.com

**Hughes Research Labs, Malibu, CA

***EMCORE Corp. Somerset, NJ

****Arizona State University, Tempe, AZ

ABSTRACT

in situ Spectroscopic Ellipsometry (SE) is an optical technique which is well suited for the monitoring of epitaxial semiconductor growth, due to its high surface sensitivity and non-invasive nature. In this work, SE systems were installed on both MBE and MOCVD deposition systems to monitor the epitaxial growth of $\text{In}_x\text{Ga}_{1-x}\text{As}$ and $\text{In}_x\text{Al}_{1-x}\text{As}$ compounds on InP substrates. The structures grown include thick lattice matched $\text{In}_{0.53}\text{Ga}_{0.47}\text{As}$ buffer layers (for HBT collectors), and strained RTD structures. SE was used to monitor in real-time layer composition and thickness during growth. To enhance the precision and accuracy of the SE determined growth parameters, it was necessary to optimize the SE data analysis strategies. A methodology to determine the best spectral region for the SE data analysis in the presence of noise and systematic effects (such as angle of incidence uncertainty, detector wavelength shifts, surface roughness, uncertainty in surface temperature, non-ideal growth modes, etc.) is presented. Using the optimized data analysis strategies, long term SE-determined $\text{In}_x\text{Ga}_{1-x}\text{As}$ composition accuracy (as verified by *ex situ* x-ray measurements) of ± 0.002 in 'x' was achieved. SE thickness measurements of ultra-thin ($< 30\text{\AA}$) strained AlAs barrier layers were also in excellent agreement ($\pm 0.5\text{\AA}$) with real-time photo-emission oscillation measurements.

INTRODUCTION

Ellipsometry is an optical technique which measures the change in polarization state of light induced by reflection from the measurement sample¹. Traditionally, Psi (Ψ) and Delta (Δ) parameters are used to report the results of the ellipsometric measurement, as quantified by (1).

$$\tan(\Psi) \cdot e^{i\Delta} = \rho = \frac{r_p}{r_s} \quad (1)$$

In equation (1), r_p and r_s are the complex reflectivities for p- and s- polarized light, and ρ is the complex reflectivity ratio for p- to s- light. Ellipsometry has some unique advantages when compared to other optical techniques such as reflection. First, since a ratio is measured (as opposed to an absolute value), extremely accurate and stable measurements can be made. Secondly, the Δ 'phase' parameter is highly sensitive to surface effects, down to the sub-monolayer level. And finally, since ellipsometry measures a complex quantity, it is possible to directly transform Ψ and Δ into the complex dielectric function of the material by using equation (2), with ρ defined in (1). To use this equation, the angle of incidence ' ϕ ' must be accurately

Cambridge University Press

978-1-107-41356-6 - In Situ Process Diagnostics and Intelligent Materials Processing

Edited by Peter A. Rosenthal, Walter M. Duncan and John A. Woollam

Excerpt

[More information](#)

known, and no films or overlayers can be present on the material. This transform is often used even when preceding assumptions are not rigorously satisfied, and the resulting dielectric function is then referred to as the pseudo-dielectric function, which is denoted $\langle \epsilon \rangle$. The ability of ellipsometry to directly measure the dielectric function is very important, as most data analysis algorithms require accurate dielectric function libraries of the materials being analyzed.

$$\epsilon = \epsilon_0 \sin(\phi)^2 \left[1 + \tan(\phi)^2 \left(\frac{1-\rho}{1+\rho} \right)^2 \right] \quad (2)$$

With spectroscopic ellipsometry (SE), the ellipsometric measurement is performed over a range of wavelengths, which provides a data set with increased information content. However, since SE only measures Ψ and Δ parameters vs. wavelength, it is necessary to perform an analysis of the data to extract other sample properties. The methodology for performing such an analysis is detailed elsewhere²⁻⁴. The general approach is to build an optical model representing the sample and use a regression algorithm to 'fit' the ellipsometric data calculated by the optical model to the experimentally measured data. A very key aspect in building an optical model is the availability of accurate dielectric function libraries. Approaches for acquiring such dielectric function libraries will be discussed in a subsequent section. Choosing the appropriate fitting parameters for the optical model, and spectral range of SE data for the fit, are also critical in obtaining an optimal analysis of the SE data. A systematic study of these effects is also presented.

In spite of the data analysis requirements imposed by the indirect nature of the measurement, Spectroscopic Ellipsometry (SE) has been successfully applied by many groups to study semiconductor growth *in situ*^{5-11,23}. Parameters which are highly relevant to the quality and reproducibility of the epitaxial growth such as surface temperature, layer thickness, and layer composition, have been extracted from the analysis of SE data. In some cases, this analysis has been performed in real-time, and controlled growth, using SE as a composition and/or thickness feedback sensor, has even been reported. However, little work has been reported on the absolute accuracy of the ellipsometrically determined growth parameters, or on the long term reproducibility of the technique. These important issues must be quantified before *in situ* SE can be relied upon as a standard diagnostic tool for epitaxial semiconductor growth. In this paper, recent results of using *in situ* SE to monitor $\text{In}_x\text{Ga}_{1-x}\text{As}$ and $\text{In}_x\text{Al}_{1-x}\text{As}$ composition and ultra thin AlAs layer thickness will be presented. The development of optimal SE analysis approaches, and comparison of the SE measurement results with other diagnostic techniques over multiple growth runs will be emphasized.

EXPERIMENT

Deposition Systems

Acquiring *in situ* SE data during epitaxial semiconductor growth requires a deposition system with optical access to the sample (typically at 70-80° angle of incidence with respect to the sample normal). This work was performed on two MBE machines (a modified Fisons V80H with inline sample manipulator and ellipsometer viewports at 75° angle of incidence, and a DCA 450 with ellipsometer viewports at 73°), and two MOCVD reactors (EMCORE GS3300 with viewports at 72.8°). Studna windows¹² were used in all installations to reduce the effect of window birefringence on the ellipsometric data. The instrument calibration algorithm¹³ was

Cambridge University Press

978-1-107-41356-6 - In Situ Process Diagnostics and Intelligent Materials Processing

Edited by Peter A. Rosenthal, Walter M. Duncan and John A. Woollam

Excerpt

[More information](#)

extended to monitor one component of the window birefringence¹⁴ (the other component combines indistinguishably with the sample's Δ parameter). It was found that the window birefringence was non-zero and on the order of a few tenths of a degree for most of the installations.

To ensure uniformity of the deposition, substrate rotation is required throughout the growth run. This can induce wobble in the ellipsometer beam which is reflected off the rotating sample surface. To reduce the residual wobble on the V80H MBE system (which could be $>0.5^\circ$), a custom sample mounting block was designed which enabled a precise *ex situ* adjustment of the wafer tilt. By measuring the wafer wobble *in situ*, the magnitude and direction of wafer tilt required to compensate the wobble could be calculated and precisely set in an *ex situ* alignment jig. Once the wafer tilt was set, beam wobble during substrate rotation of less than 0.1° was routinely achieved. This reduction in beam wobble significantly improved the ellipsometer signal/noise, and was an important factor in improving the absolute composition accuracy achieved by the SE system. The DCA sample manipulator incorporated piezoelectric crystals into the design, such that any beam wobble could be nulled out *in situ* by adjusting the voltages across the crystals in real-time.

The EMCORE MOCVD reactors employ a TurboDisc technology in which the substrate spins at a very high rotation rate (800 rpm in this work). The beam wobble in such a system is by necessity quite low, such that ellipsometric measurements can be easily performed during growth. For most of this work, a single wafer platter was used in the reactor, although accurate ellipsometric data was also acquired on a 3 wafer platter (as long as 3 good wafers were grown on).

Spectroscopic Ellipsometer Hardware

Commercially available multi-wavelength ellipsometer systems, based on the rotating analyzer configuration, were used in this work¹⁵. Three of the installations used 88 channel systems with a spectral range of 280-760 nm, and one of the installations used a 44 channel system with a spectral range of 420-760 nm. To achieve good signal/noise in the SE data, a data acquisition time equal to the substrate rotation period of 4.5 seconds was used on the MBE systems. On the MOCVD reactors in which the substrate rotated at a much higher rate, the data were averaged over multiple revolutions of the substrate, with a typical acquisition time of 2-5 seconds. To obtain the highest possible data accuracy and partial cancellation of window birefringence effects, zone averaged ellipsometric measurements¹⁴ were performed throughout the growth run, except during the growth of very thin layers.

SE Data Analysis Software

Analysis of the SE data was performed both in real-time and off-line using commercially available software¹⁶. This software performs standard optical modeling and regression analysis as discussed in the literature¹⁴. To simplify the analysis of *in situ* SE data, the 'virtual interface' approximation was employed¹⁷⁻¹⁹, which is essentially exact for optical data acquired during epitaxial semiconductor growth. The virtual interface analysis approach is illustrated in Figure 1. The concept is quite simple: a simplified optical model for the sample is built by replacing the past growth history with a single 'pseudo substrate' layer. The pseudo dielectric function of this layer is obtained by transforming the ellipsometric data measured at the corresponding growth time via equation (2). The simplified optical model can then be used to determine the film thickness, composition, etc. of the recent film growth, independent of the underlying sample

complexity. Since exact Fresnel and thin film interference expressions may be used in calculating the predicted ellipsometric response of the simplified optical model, there are no limitations on the layer thicknesses which can be analyzed with this approach (with the obvious exception that as the film becomes optically thick, i.e., the light does not penetrate the depth of the layer, it is not possible to directly measure the film thickness; it may however in this case be sufficient to extrapolate the film thickness from the SE-determined initial layer growth rate).

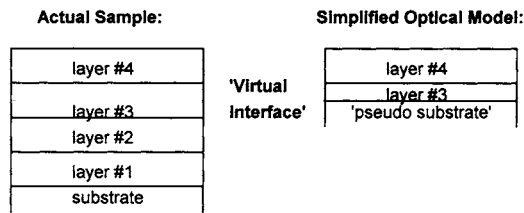


Figure 1. Virtual Interface approach used to simplify SE data analysis.

With the exception of the substrate characterization results, all of the SE data analysis performed in this work utilized some variation of the virtual interface approach^{7,10}. In some cases, the virtual interface was located at the layer interface (to determine layer thickness), and in other cases, the virtual interface was dynamically tracked to include only the most recent 'n' data points in the analysis (to determine the near surface composition, morphology, etc.). Other parameters which must be optimized in the analysis are: the number of time slices and spectral range of experimental data included in the regression analysis, and the model fit parameters, which can include thickness, growth rate, angle of incidence, composition, surface roughness, and surface temperature.

Dielectric Function Libraries

As previously mentioned, accurate dielectric function libraries are required to perform real-time analysis of *in situ* SE data. Fortunately, it is possible to directly measure such libraries via SE. Measuring a substrate dielectric function library vs. temperature is fairly straightforward: 1) the substrate is measured *in situ* at room temperature, and an optical model using a reference dielectric function spectra from the literature is used to determine the angle of incidence ϕ and the oxide thickness, 2) the substrate temperature is ramped to remove the oxide, and a buffer layer is grown (if possible) to produce an atomically smooth surface, 3) the temperature is systematically ramped while SE data is acquired at the different substrate temperatures, 4) equation (2) is used to extract dielectric function spectra from the *in situ* SE at the various temperatures, and 5) the temperature dependent dielectric function spectra are assembled into a library file.

The purpose of the library file is to generate substrate dielectric function spectra at arbitrary temperatures; this capability is required for subsequent real-time analysis of SE data. In this work, the dielectric function spectra vs. temperature was parameterized into a temperature dependent library by fitting a low order polynomial in temperature to the dielectric function data at each measured wavelength; the resulting polynomial coefficients could then be used to generate a substrate dielectric function spectra at an arbitrary temperature. (This same approach was used to parameterize composition dependence as well.) The main advantage of using

polynomials is simplicity; a critical point shifting algorithm²⁰ or other more sophisticated parameterization schemes²¹ could also be used to generate an dielectric function library.

Acquiring a dielectric function library for a ternary semiconductor system is more involved. In general it is necessary to acquire a library which contains both temperature and composition dependence. Furthermore, it is important to acquire the dielectric function library under actual growth conditions, for two reasons: 1) these are the conditions under which subsequent SE real-time monitoring will be utilized, and 2) the surface morphology/chemistry of the material, and therefore its dielectric function, may change under static vs. growing conditions. Figure 2 shows direct evidence of the change in ellipsometric data for a growing (via MBE, at T=450C) vs. static $\text{In}_{0.53}\text{Ga}_{0.47}\text{As}$ surface. The exact nature of the surface change can not be concluded from SE alone (it can be qualitatively optically modeled by a decrease in surface roughness of about 1 Å), but the effect is optically significant, and must be considered when acquiring and analyzing *in situ* SE data. This effect was not observed in MOCVD growth (at T=650C) of $\text{In}_{0.53}\text{Ga}_{0.47}\text{As}$, which may offer evidence of differing growth kinetics between MBE and MOCVD grown $\text{In}_x\text{Ga}_{1-x}\text{As}$.

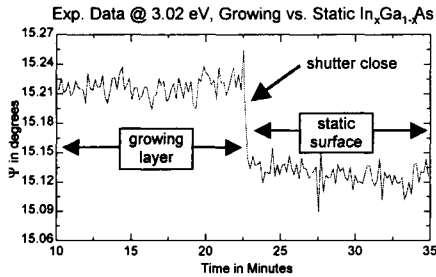


Figure 2. Raw ellipsometric Ψ data (at a selected wavelength) illustrating the change in data for a growing vs. static $\text{In}_{0.53}\text{Ga}_{0.47}\text{As}$ surface.

Special growth structures were designed to efficiently acquire a temperature and composition dependent dielectric function library in a single growth run. Since a primary goal of this work was to grow only lattice matched compositions of $\text{In}_x\text{Ga}_{1-x}\text{As}$ and $\text{In}_x\text{Al}_{1-x}\text{As}$ on InP (the lattice match compositions are $x=0.532$ and $x=0.522$ respectively), it was determined that a full grid of composition and temperature dielectric function spectra were not required. Instead, multiple compositions were grown at a single temperature, and at a single composition (the lattice match value) multiple temperatures were grown. Figure 3 illustrates such a growth structure for $\text{In}_x\text{Al}_{1-x}\text{As}$, and the raw SE data acquired during the growth of this structure are shown in Figure 4 (similar structures were also grown for $\text{In}_x\text{Ga}_{1-x}\text{As}$, and both in the MBE and MOCVD systems). The oscillations present in the data are due to thin film interference effects, which are caused by the slight difference in dielectric function for each of the different compositions. Dielectric function spectra for each composition were obtained by fitting all the ellipsometric data vs. time measured during the growth of each layer, assuming a constant growth rate. Distinct peaks corresponding to each layer were observed in the x-ray diffraction spectra, and were used to assign accurate composition values to each spectra. In the MBE environment, an absorption band-end spectroscopy (ABES) temperature sensor²² was used to precisely control the temperatures throughout the run, while in the MOCVD systems, the substrate thermocouple reading was used.

T=500	1200Å	} x=0.523
T=540	1200Å	
T=520	1200Å	
T=500	1200Å	
T=480	1200Å	
T=460	1200Å	} T=500
x=0.523	2000Å	
x=0.543	2000Å	
x=0.533	2000Å	
x=0.503	2000Å	
x=0.513	2000Å	
x=0.523	2000Å	
InP Substrate		

Figure 3. Growth structure to acquire composition and temperature dependent dielectric function library.

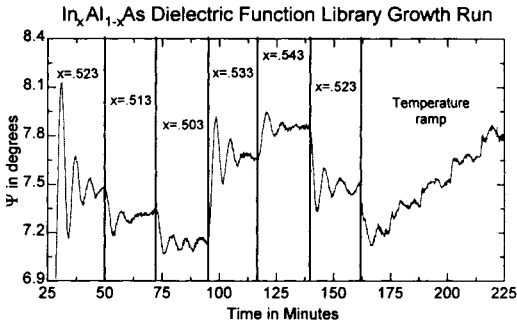


Figure 4. Raw *in situ* SE data acquired during the growth of the structure shown in Figure 3 (shown at a selected wavelength).

The dielectric function library measured for MBE-grown $\text{In}_x\text{Ga}_{1-x}\text{As}$ is shown in Figures 5 and 6. On the scale of these plots, the change in dielectric function vs. composition and temperature appears to be quite small, especially for composition. Figure 7 more directly illustrates the dielectric function sensitivity to composition, by plotting the change in ϵ for a 0.01 change in composition. For comparison, the sensitivity curves for $\text{In}_x\text{Ga}_{1-x}\text{As}$, $\text{In}_x\text{Al}_{1-x}\text{As}$, and $\text{Al}_x\text{Ga}_{1-x}\text{As}$ are all plotted together. From the plots in Figure 7 it is very obvious that the composition sensitivity for $\text{In}_x\text{Ga}_{1-x}\text{As}$ is 2-4 times less than that of $\text{In}_x\text{Al}_{1-x}\text{As}$ and $\text{Al}_x\text{Ga}_{1-x}\text{As}$. This implies that $\text{In}_x\text{Ga}_{1-x}\text{As}$ is a particularly challenging material for real-time composition monitoring by *in situ* SE. (A typical lattice matching specification, which dictates the required absolute accuracy of the SE composition determination, is ± 0.005 in 'x'.)

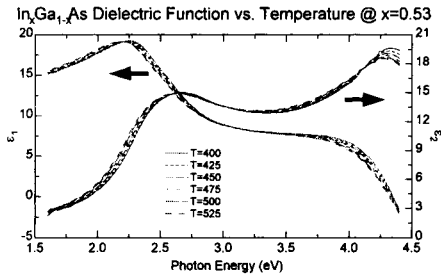


Figure 5. MBE-grown $\text{In}_x\text{Ga}_{1-x}\text{As}$ dielectric function vs. temperature at $x=0.53$.

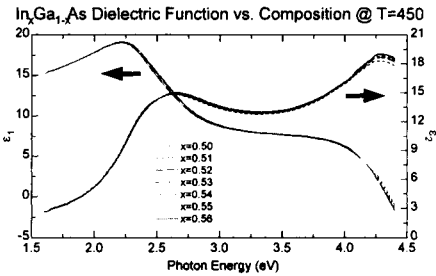


Figure 6. MBE-grown $\text{In}_x\text{Ga}_{1-x}\text{As}$ dielectric function vs. composition at $T=450\text{C}$.

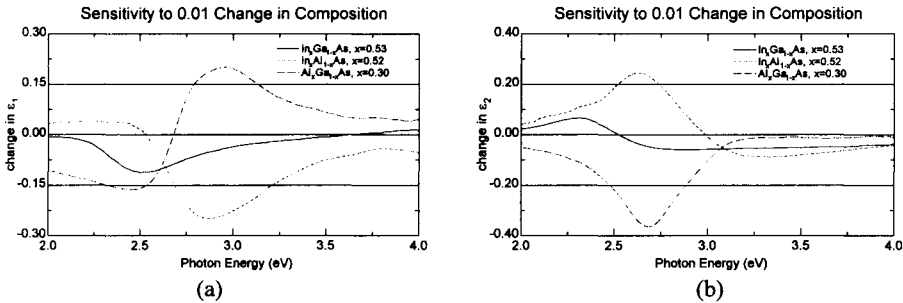


Figure 7. Changes in the real (a) and imaginary (b) dielectric functions of $\text{In}_x\text{Ga}_{1-x}\text{As}$, $\text{In}_x\text{Al}_{1-x}\text{As}$, and $\text{Al}_x\text{Ga}_{1-x}\text{As}$ induced by a 0.01 change in 'x'

SE Sensitivity to Composition and Systematic Perturbations

In Figure 8, the composition sensitivity of $\text{In}_x\text{Ga}_{1-x}\text{As}$ is compared relative to other systematic perturbations which may be present in the *in situ* environment. These include angle of incidence uncertainties, surface roughness, substrate temperature uncertainties, and wavelength calibration inaccuracies of the SE detector system. The SE sensitivity to these effects is comparable to the SE composition sensitivity. However, since each effect has a characteristic spectral dependence, it may be possible to select an optimum spectral range for data analysis that minimizes the impact of specific systematic perturbations on the SE composition accuracy. In Table I, the composition was extracted from simulated SE data sets which were systematically perturbed. From this table, it is clear that the composition error is dependent on the spectral range used in the SE data analysis and the type and magnitude of systematic perturbations. In the bottom row, the square root of the sum of the squares of the composition errors due to all of the perturbations are reported. These values may be used to objectively select an optimum spectral range for the SE data analysis (in Table I, 3.0-3.7 and 2.0-4.0 appear to be the best choices). However, this estimation is based upon the assumed magnitudes for the various perturbations; the best way to optimize the spectral range is by reanalyzing actual SE experimental data from multiple growth runs, which is investigated in the next section.

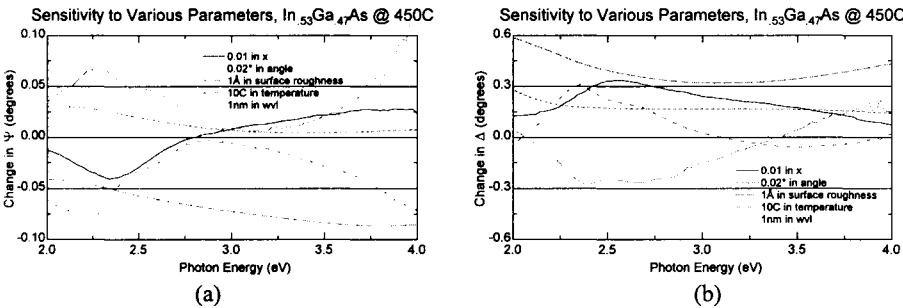


Figure 8. Calculated changes in the ellipsometric Ψ (a) and Δ (b) data for perturbations of: 0.01 in composition, 0.02° in angle, 1Å in surface roughness, 10C in temperature, and 1nm in wavelength shift. (A substrate of $\text{In}_{0.53}\text{Ga}_{0.47}\text{As}$ at 450C and 75° angle of incidence is used for the starting optical model.)

Table I. Error in $\text{In}_x\text{Ga}_{1-x}\text{As}$ composition induced by systematic perturbations, using various spectral ranges for the SE data analysis.

Systematic Perturbation	Selected Spectral Range (in eV)					
	1.6 - 2.3	2.3 - 3.0	3.0 - 3.7	3.7 - 4.4	1.6 - 4.4	2.0 - 4.0
0.02° in angle of incidence	-0.009	0.004	0.008	0.013	0.005	0.005
1Å in surface roughness	0.021	0.013	0.013	0.022	0.016	0.014
10C in substrate temperature	0.016	0.007	-0.005	-0.004	0.005	0.005
1nm in wavelength shift	-0.010	-0.013	0.000	-0.012	-0.010	-0.007
'Uncorrelated' sum of effects:	0.030	0.020	0.016	0.028	0.020	0.017

RESULTS

Observation of Interface Effects by *in situ* SE

When the epitaxial growth of a semiconductor layer is initiated, a simple optical model (consisting of a uniform film growing at a constant rate with an abrupt interface) should adequately describe the *in situ* SE data. This is illustrated in Figure 9, in which an $\text{In}_{0.53}\text{Ga}_{0.47}\text{As}$ layer is grown on an InP substrate by MOCVD. However, for some material interfaces, non-ideal behavior was observed in the *in situ* SE data, as depicted in Figure 10 for the growth of $\text{In}_{0.52}\text{Al}_{0.48}\text{As}$ on InP by MOCVD. This implies the existence of a non-abrupt interface, which was confirmed by XTEM measurements (interface non-idealities were also observed by *in situ* SE for MBE growth of these materials). Therefore, interface quality is yet another parameter to which *in situ* SE is sensitive, and since it is difficult to quantitatively model the interface effects in real-time, it should be treated as another systematic perturbation which can degrade the SE composition accuracy. In the next sections, SE data acquired near the interface region was excluded from the composition accuracy analysis.

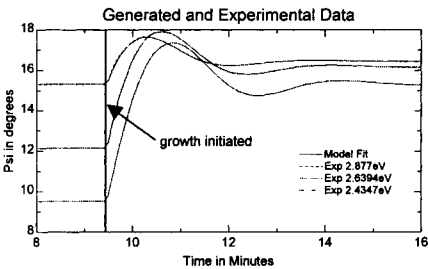


Figure 9. *in situ* SE data from an $\text{In}_{0.53}\text{Ga}_{0.47}\text{As}$ layer grown on InP by MOCVD; note the near perfect model fit.

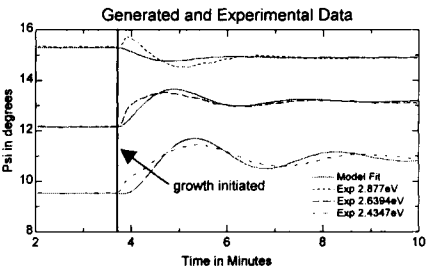


Figure 10. *in situ* SE data acquired from a $\text{In}_{0.52}\text{Al}_{0.48}\text{As}$ layer grown on InP by MOCVD; note the poor quality of the data fit.

Optimizing the SE Data Analysis for InGaAs Composition

To determine the optimum SE data analysis strategy, 6 growth runs which encompassed 18 $\text{In}_x\text{Ga}_{1-x}\text{As}$ layers were analyzed using different spectral ranges and fitting parameters. The